Temperature and Concentration Measurements in a Solid Fuel Ramjet Combustion Chamber

G. Schulte,* R. Pein,† and A. Högl†
Institute for Chemical Propulsion and Engineering, Hardthausen-Lampoldshausen, Federal Republic of Germany

The combustion of solid fuels has been studied by using a solid fuel ramjet combustion chamber equipped with a vitiated air heater. The fuels were polyethylene (PE) and hydroxyl-terminated polybutadiene (HTPB), with PE being the prevailing fuel. The air was heated by combustion of hydrogen and oxygen. In order to get a better understanding of the combustion process, a thermocouple and a gas-chromatographic technique were used to obtain temperature and species concentration profiles throughout the combustion chamber. The measurements were taken at several axial and radial positions of the combustion chamber, including measurements in the recirculation zone of the flameholder and in the afterburner chamber. The influence of different test conditions, like mixture ratio, inlet temperature, and mass flux, was also investigated. The results are discussed with regard to flame position, turbulent mixing, and combustion efficiency.

Nomenclature

A = area
D = diameter
d = wire diameter
G_{air} = air mass flux, $\dot{m}/A_3$
$\dot{m}$ = air mass flow
O/F = mixture ratio air/fuel
p_c = combustion pressure
r = radius
$\bar{r}$ = average regression rate
T = temperature
w = velocity
z = axial coordinate
ϵ = emissivity of the thermocouple probe
η = viscosity
λ = thermal conductivity
ρ = density
σ = Stefan-Boltzmann constant
ϕ = equivalence ratio $(O/F)_{stoich.}/(O/F)$

Subscripts

2 = flameholder inlet
3 = fuel port
4 = afterburner chamber
5 = nozzle throat
a = axial coordinate of afterburner chamber
b = thermocouple bead
r = radiation
w = wall
tot = total

Introduction

SOLID fuel ramjets may be potential missile propulsion systems for the future. Their advantages are simplicity and light construction, the use of air from the atmosphere as oxidizer, and the absence of fuel tankage, control, and delivery systems. The fuels are just nonexplosive polymers.

Several authors[1-5] have investigated the combustion of solid fuels in a ramjet combustion chamber. Most of these studies investigated the influence of various parameters like chamber pressure and mass flux on the fuel regression rate. Other researchers[6-11] have established theoretical models of ramjet combustion. In this connection, the theoretical and experimental publications on hybrid combustion[12,13] are also very interesting, since there is a close relationship between ramjet and hybrid combustion. However, few authors have measured temperature and species distributions in a solid fuel ramjet combustion chamber. Schadow et al.[14] gave some detailed results for various test conditions, but species concentration measurements were only made in the afterburner chamber, not in the combustion channel. Of course, there are many publications in the literature concerning the combustion of polymers,[15-17] but in most cases the experimental circumstances are very different from those in a ramjet combustion chamber. Nevertheless, such studies can be very helpful in understanding the ramjet combustion process. Studies on turbulent boundary layers with porous wall injection and combustion as performed by Wooldridge et al.[18] and others[19,20] are also valuable for elucidation of ramjet combustion problems. A lot of these works have especially emphasized the velocity profiles.

The object of this study was to make an effort to perform measurements of the temperature and concentration fields directly in a solid fuel ramjet combustion chamber, since there is not much information in this field. The measurements were done by means of thermocouple and gas-chromatographic techniques. The combustion in a solid fuel ramjet is not stationary because of combustion channel expansion by fuel regression. Therefore, the existing techniques had to be adapted to this situation. The concentration measurements were restricted to the main combustion species: CO, CO_2, H_2, H_2O, N_2, and O_2. The influence of stoichiometry, mass flux, inlet temperature and fuel was studied, using a combustion chamber which has been connected to a hydrogen/oxygen air heater. The results of these measurements should lead to a better understanding of the combustion process.

Experimental Hardware

Combustor Setup and Test Conditions

The combustor and the air heater are shown schematically in Fig. 1. The air is heated through the combustion of hydrogen and oxygen. Oxygen is replenished, so that the

Received March 25, 1986; revision received Aug. 7, 1986.

*Aerospace Engineer.
†Chemical Engineer.

amount of oxygen is kept constant at 21 vol % of the total air massflow. The amount of water vapor in the air depends on the desired air temperature (e.g. $T_{2,\text{tot}} = 200°C$: water vapor = 3 vol %). All tests were carried out at an initial port diameter for the fuel grain of 60 mm. The standard fuel in this study was PE. The test conditions, under which temperature and species concentration measurements were undertaken, are given in Table 1. Chamber pressure, air mass flux, and air inlet temperature are the main parameters which influence the rate of decomposition of the solid fuel. The area ratios fuel port/injector (A_3/A_2) and fuel port/throat (A_3/A_5) describe the geometry and determine the velocity inside the combustor.

Tests at condition A were made at an air-rich mixture ratio ($\phi = 0.56$). At this condition, several temperature and concentration profiles at different axial locations inside the combustor were carried out. At test condition B, a near stoichiometric mixture ratio ($\phi = 0.96$) with a reduced air mass flux ($G_{\text{air}} = 10.9$ g/cm^2 s) was investigated. Tests at conditions C and D were made at two different air inlet temperatures ($T_{2,\text{tot}} = 0$ and 400°C). One test with a HTPB fuel was carried out (condition E).

The positions of the thermocouple and sampling probe are given in Fig. 1. The majority of the measurements were taken inside the fuel port, whereas only one cross section at the end of the afterburner chamber was investigated.

Temperature Measurements with Thermocouples

Temperature measurements were made using platinum rhodium 70/30 platinum/rhodium 94/6 (El 18) thermocouples having 0.2 mm wire diameter. With the help of a motor drive, the thermocouple was moved through the fuel grain into the combustor. The thermocouple protection tubes and the motor drive are shown in Fig. 2. During the ignition phase of the fuel grain with a H_2/O_2 hot gas igniter (torch), the thermocouple was placed inside the fuel grain. After sustained combustion was established, the thermocouple was moved inside the combustor at a constant velocity up to the center line of the fuel grain. The majority of the tests were conducted at a thermocouple velocity of 3.4 mm/s, whereas for some tests a reduced speed was applied to make sure that the response time of the thermocouple was well adapted. The voltage output of the thermocouple and the position indicator were recorded on a minicomputer. The positioning accuracy of the thermocouple bead was ± 0.1 mm. Taking into account the fuel regression, a temperature profile with respect to the actual distance to the fuel wall could be plotted. Corrections were made for radiation effects, using the following expression proposed by Kaskan[21]

$$\Delta T_r = \frac{1.25 \cdot \epsilon \cdot \sigma \cdot d^{0.75}}{\lambda} \left(\frac{\eta}{\rho \cdot w}\right)^{0.25} \left(T_b^4 - T_w^4\right)$$

The heat conduction along the wires was small compared to the convective heat transfer between the wires and the gas and could be neglected. Catalytic effects were investigated by comparing data obtained with coated and uncoated thermocouples. A mixture of yttrium and beryllium oxide was used for the coating.[22,23]

Gas Chromatography Setup and Evaluation Procedure

The concentration measurements were undertaken by modifying the method of Banna and Branch.[24] Because the concentration of species in a ramjet combustion centration chamber is dependent on time and location, any gas sampling has to be done in a very short time period. The sampling time was about 2-3 s in study. Thus, the burning channel diameter remained nearly constant during one measuring period. The gas samples were taken from the combustion chamber by a small water-cooled probe of an internal diameter of 0.6 mm and an external diameter of 3 mm. The probe was inserted into a hole drilled through the fuel block. The gas sampling arrangement is shown in Fig. 3. In order to avoid too early entering of combustion gas, the probe was purged with helium prior to sampling. This purge was needed because the pressure in the combustion chamber was higher than the pressure in the sampling arrangement. The probe was connected to a helium lecture bottle and to the rest of the experimental setup via a 3-port valve. The rest of the setup consisted of a soot filter, a silica gel trap for water removal, and a gas sampling cylinder. The lines up to the 3-port valve and the cylinder were evacuated. The lines from the probe up to the silica gel tube were heated by insulated heating wire in order to avoid any condensation of water. After each test run, the sampling cylinder was connected to the injection valve of a gas chromatograph equipped with a thermal conductivity detector. The gases were analyzed for N_2, O_2, CO, CO_2 and H_2 and were separated by a Porapak T and a molecular sieve 5A column. Calibration gases were obtained by a partial pressure procedure. H_2O was determined by weighing the silica gel tube or by a mole balance.

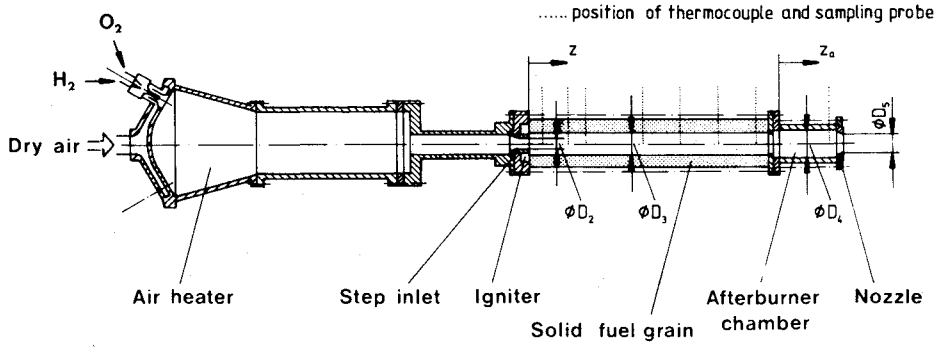

Fig. 1 Schematic arrangement of SFRJ combustor and air heater.

Table 1 Test conditions

Test condition	p_c/bar	G_{air}/(g/cm^{2}s)	$T_{2,\text{tot}}$/(°C)	ϕ	A_3/A_5	A_3/A_2	Fuel
A	5.2	30.0	200	0.56	1.86	4.09	PE
B	5.9	10.9	190	0.96	3.78	6.39	PE
C	5.4	30.0	0	0.42	1.97	4.59	PE
D	5.9	30.7	400	0.69	1.60	3.52	PE
E	5.8	29.5	190	1.00	1.60	3.52	HTPB

No attempt was made to apply isokinetic sampling. Turbulent fluctuations, recirculating flow, and combustor geometry make the meaning of isokinetic sampling questionable in this case.

Test Results and Discussion

Temperature and species concentration measurements will be presented as radial profiles at different axial positions of the fuel grain and at one position in the afterburner chamber. Because of axisymmetric combustor geometries, it can be assumed that temperature and concentration profiles are axisymmetric, too. The axial position of the measurements in the combustor are characterized by z/D_3, where z is the axial distance measured in the streamwise direction of the fuel grain, and D_3 is the initial fuel port diameter. The afterburner axial position is characterized by z_a/D_4, where z_a is the distance from the downstream end of the fuel grain and D_4 the afterburner diameter.

Temperature Profiles

The radial temperature profiles in the combustor for test condition A are shown in Figs. 4 and 5. In Fig. 4, profiles at three axial positions in the area of the recirculation zone are presented. The first profile downstream of the flameholder step ($z/D_3 = 0.6$) shows a rapid increase of the air inlet temperature to a maximum temperature of approximately 1600°C. Going further downstream, the peak temperature approaches to the solid wall and the mixing process increases. These three profiles show that the combustion process takes place mainly in the shear layer of the incoming air flow and the recirculation zone. In Fig. 5, four temperature profiles downstream of the recirculation zone are presented. In this part of the combustor, the maximum temperatures occur very close to the fuel wall and have a similar development over the cross section. With increasing axial position, the temperature peak near the wall and the temperatures in the middle of the fuel port both increase. In Fig. 6, two temperature profiles at two axial positions with different air mass fluxes are compared. The reduction of the air mass flow ($G_{air} = 10.9$ g/cm²s) and the decrease of the throat cross section ($A_3/A_5 = 3.78$) in comparison to condition A reduce the axial velocity in the combustor and, at the same time, the fuel regression rate diminishes. However, because the decrease of the regression rate is weaker than the reduction of the air mass flux, the fuel can penetrate deeper into the airstream and, therefore, the distance of the maximum temperature from the wall increases.

At high G_{air} (condition A), the flame region with the highest temperature has a distance of about 2.5 mm from the wall, whereas at low G_{air} (condition B) the distance is about 5 mm. This effect has also been observed by Schadow et al.[14] and is in accordance with theoretical models. The corresponding dependence of the regression rate on the air mass flux is shown in Fig. 7.

An additional test series was conducted to investigate the effect of air inlet temperature. For a constant axial position ($z/D_3 = 8.3$), three radial temperature profiles are presented in Fig. 8. With increasing $T_{2,tot}$ the maximum temperature near the wall and the temperature level in the middle of the combustor increase. The distance between the maximum temperature and the wall slightly increases with $T_{2,tot}$. In Fig. 9, the corresponding regression rate vs air inlet temperature is shown. The regression rate dependence on the air inlet temperature ($\bar{r} \sim T_{2,tot}^{0.56}$) is somewhat stronger than on the air mass flux ($\bar{r} \sim G_{air}^{0.37}$).

For test conditions A and B, two radial temperature profiles at the rear end of the afterburner chamber ($z_a/D_4 = 1.7$) are shown in Fig. 10. The radial temperature profile for con-

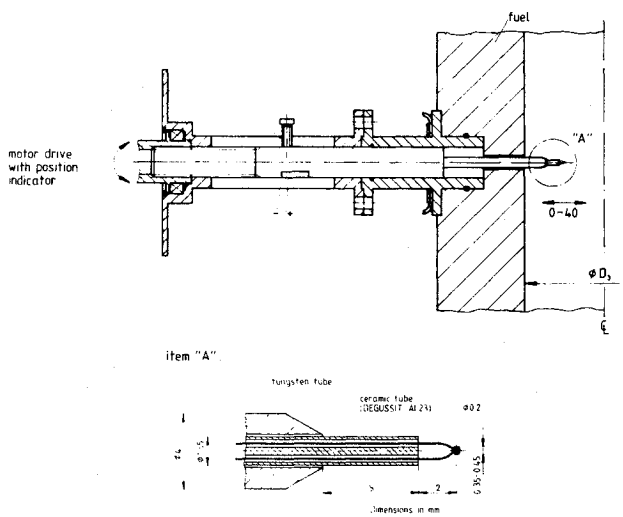

Fig. 2 Thermocouple probe and motor drive.

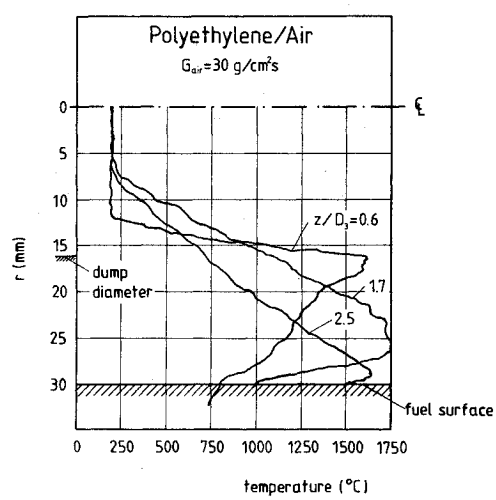

Fig. 4 Radial temperature profiles in the recirculation zone (test condition A).

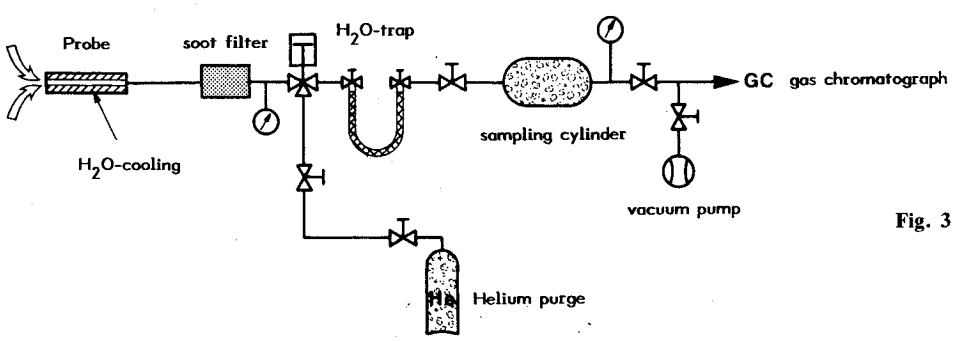

Fig. 3 Experimental facility for gas sampling.

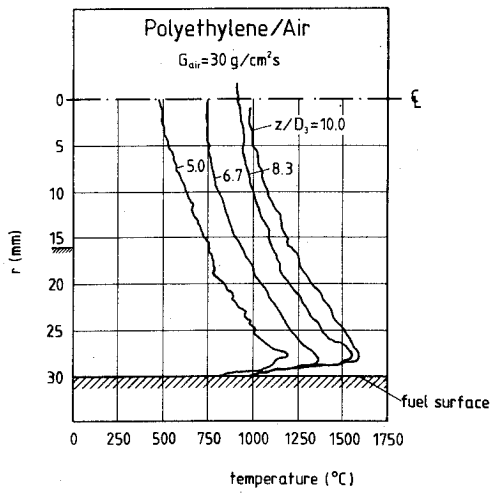

Fig. 5 Radial temperature profiles downstream of the recirculation zone (test condition A).

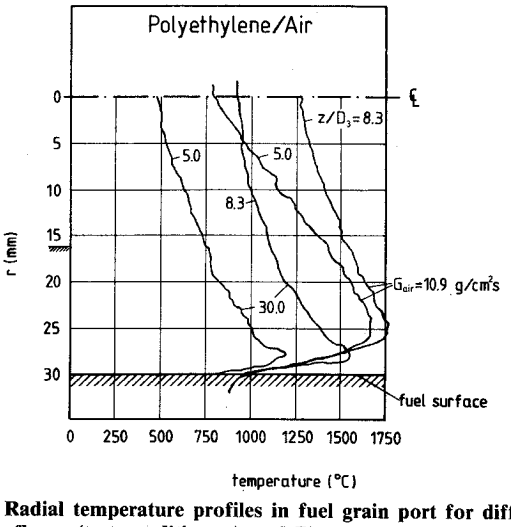

Fig. 6 Radial temperature profiles in fuel grain port for different air mass fluxes (test conditions A and B).

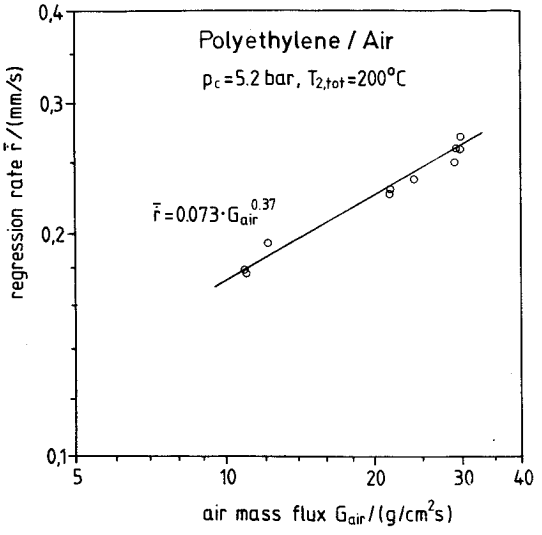

Fig. 7 Regression rate vs air mass flux.

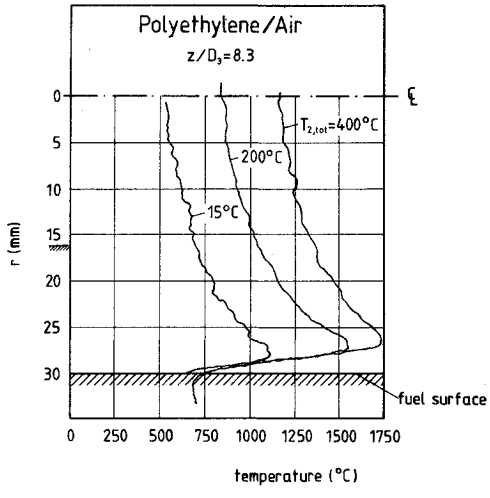

Fig. 8 Radial temperature profiles in fuel grain port for different air inlet temperatures (test conditions A, C, D).

dition B is nearly constant, and at test condition A the profile shows more temperature variations. The better mixing in case B may be explained by the lower velocities inside the combustor. The corresponding temperature profiles at the end of the fuel grain port ($z/D_3 = 10$) can be seen in Fig. 6. The adiabatic flame temperatures of the test conditions A ($\phi = 0.56$) and B ($\phi = 0.96$) are indicated in Fig. 10. In case A, the mixing process is not complete, but the reaction seems to be finished because the theoretical temperature agrees with the average experimental temperature. The near stoichiometric mixture ratio of test condition B has a higher adiabatic flame temperature, and the combustion process still seems to be incomplete. To complete the combustion process, the length of the afterburner chamber should be increased.

In Fig. 11 the radial temperature profiles at $z/D_3 = 8.3$ are shown for two different fuel types (PE—test condition A, HTPB—test condition E). The test conditions are about the same but the regression rate of the HTPB-fuel is approximately 85% higher than for the PE-fuel. Therefore, the average temperature level at the same cross section is somewhat higher for the HTPB-test and the temperature maximum occurs farther from the wall.

The results of the investigation of the catalytic effects produced by the platinum-rhodium thermocouples are given in Fig. 12. The differences in temperature obtained with coated and uncoated thermocouples are not significant and are within the range of reproducibility of the tests. Therefore, the majority of the tests was conducted with uncoated thermocouples.

Combustion Chamber Concentration Profiles

The radial concentration profiles in the combustor at test condition A are presented in Figs. 13–18. Each figure shows the behavior at different axial positions of the probe. Figure 13 represents the concentration profiles across the recirculation zone at $z/D_3 = 0.6$. In the middle of the combustion chamber, the composition of the gases corresponds nearly to that of air, and no combustion products are found there. In the region closer to the wall, the oxygen concentration drops to a very low value, and the combustion products CO, CO_2, H_2O, together with N_2 are the prevailing species. The carbon monoxide concentration is high, indicating a fuel-rich combustion in the recirculation zone. All profiles except the O_2 profile show maximum values; this may be explained by the complicated transport and flow mechanism in this zone. Figure 14 shows the concentration profiles at a position closer to the end of the recirculation zone ($z/D_3 = 1.7$). In the middle, the composition is still close to that of air and only low concentrations of combustion products are found. The concentrations of CO, CO_2, and H_2O increase with

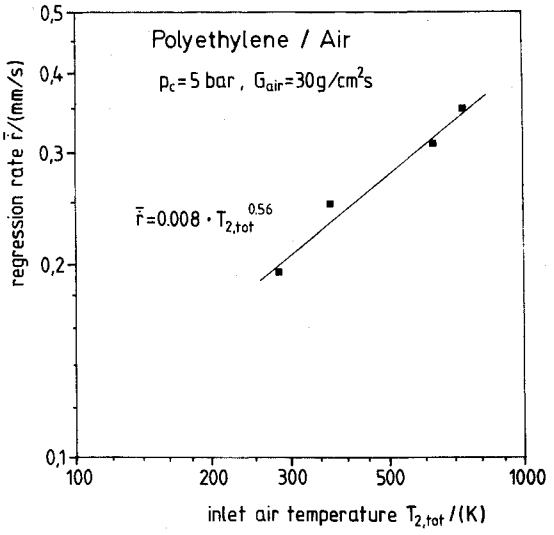

Fig. 9 Regression rate vs air inlet temperature.

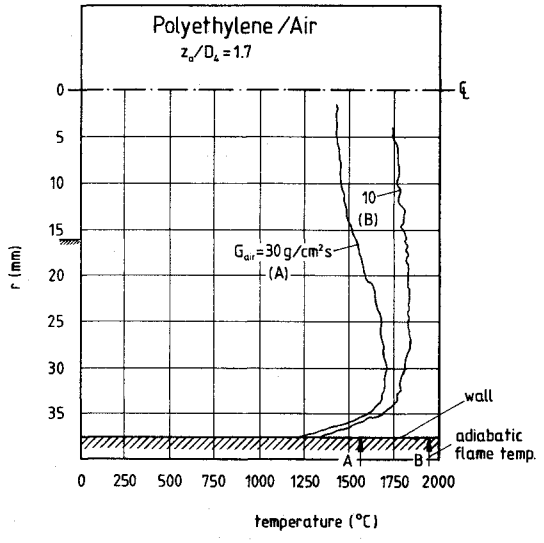

Fig. 10 Radial temperature profiles at the end of the afterburner chamber (test conditions A and B).

diminishing distance from the wall, whereas the concentrations of O_2 and N_2 decrease. There is still some oxygen at the wall; in fact, the content at and close to the wall is higher than at $z/D_3 = 0.6$. The carbon monoxide content is much lower than the content upstream. Figure 15 presents the distribution of concentrations at $z/D_3 = 2.5$ located at a transition position between the recirculation zone and the redeveloping boundary layer. The composition at the centerline is still close to the composition of the air at the inlet, but small amounts of the combustion products may also be found. The concentrations of the combustion products increase when approaching the wall, with the concentration of CO being the highest at the wall. The concentrations of O_2 and N_2 decrease from the centerline to the wall. The oxygen content at the wall is about 1.5 vol %. Figures 16 and 17 show two radial concentration profiles for all species at locations further downstream from the recirculation zone. Figure 16 indicates some significant changes in comparison to Figs. 13–15, the oxygen concentration in the middle of the combustion chamber being distinctly less than the inlet oxygen concentration. This is due to the consumption of oxygen in axial direction by the combustion process. Moreover, the concentrations of carbon dioxide and water reach higher levels at the centerline than were found upstream. These effects are more significant towards the end of the fuel grain. The situation close to the end of the fuel grain is shown in Fig. 17. The oxygen concentration at the centerline has decreased to 14 vol %, and the concentrations of CO_2 and H_2O have increased to 5.0 and 7.5%, respectively. No carbon monoxide was found in the middle of the combustion chamber; this was also observed at all other axial locations.

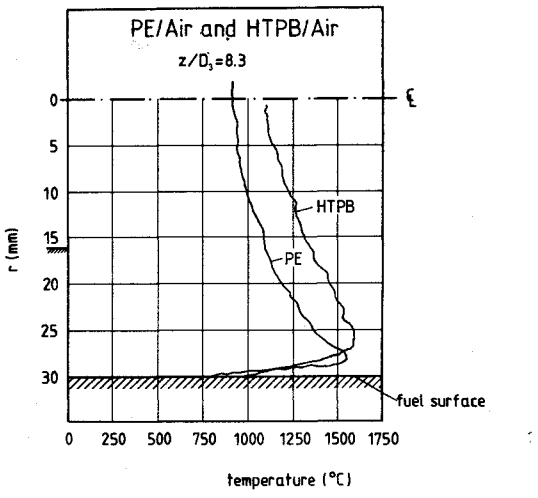

Fig. 11 Radial temperature profiles in fuel grain port (PE and HTPB fuel).

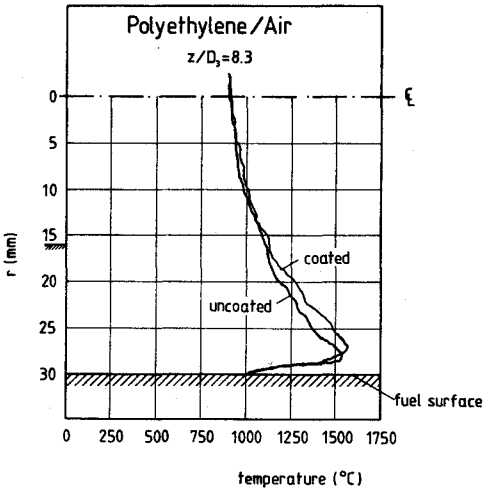

Fig. 12 Comparison of coated and uncoated thermocouple bead.

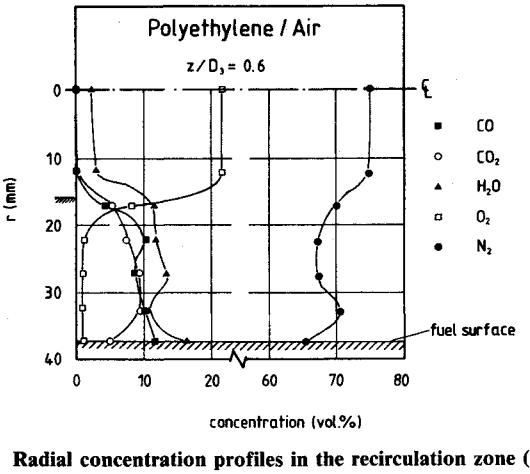

Fig. 13 Radial concentration profiles in the recirculation zone (test condition A).

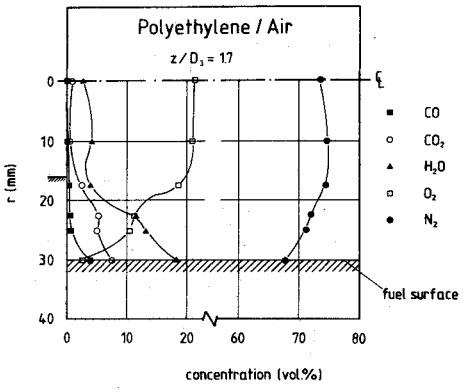

Fig. 14 Radial concentration profiles in the recirculation zone further downstream (test condition A).

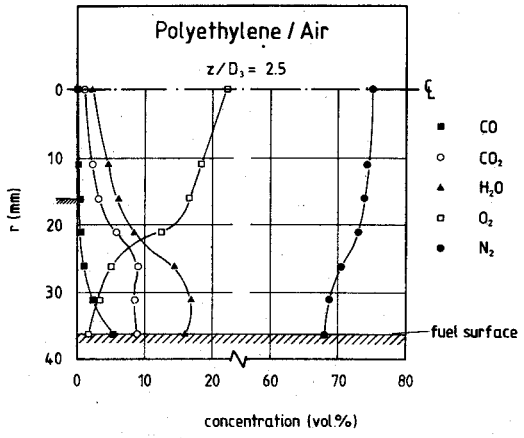

Fig. 15 Radial concentration profiles near to the reattachment point (test condition A).

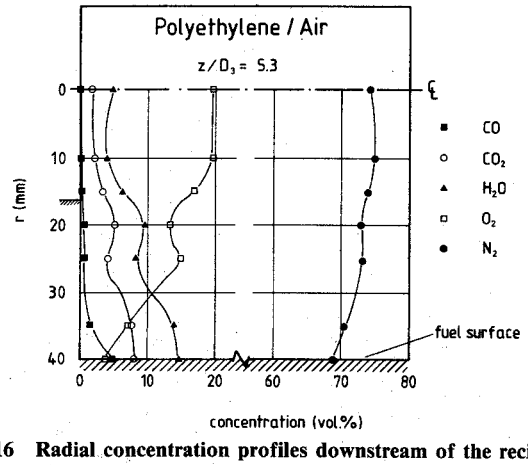

Fig. 16 Radial concentration profiles downstream of the recirculation zone (test condition A).

At the wall, the highest CO concentrations have been found. Figure 18 represents the concentration profiles at the end of the afterburner chamber at $z_a/D_4 = 1.8$. Only small amounts of carbon monoxide were found here. The concentration field is not fully homogeneous, although there is some recirculating flow at the inlet of the afterburner chamber, which should improve mixing. The oxygen concentration is much lower at the wall than in the middle. The overall mixture ratio for test condition A ($\phi = 0.56$) shows that there has to remain theoretically an oxygen concentration of about 9 vol

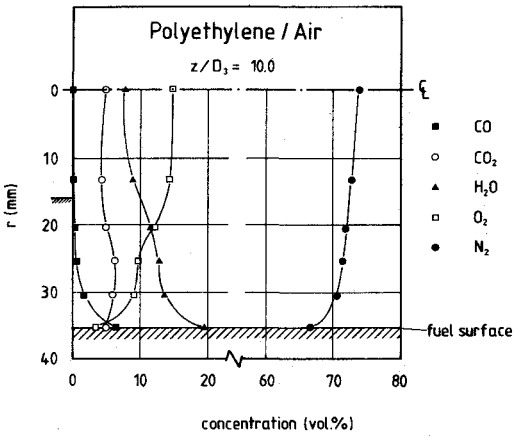

Fig. 17 Radial concentration profiles at the end of the fuel grain (test condition A).

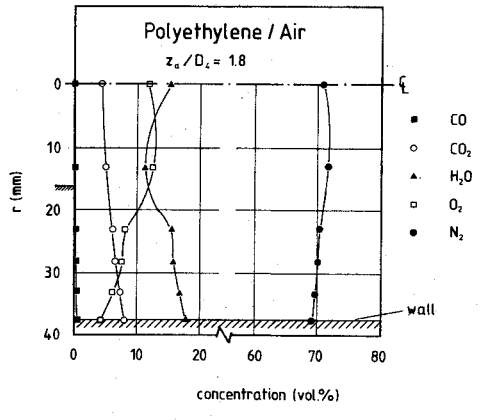

Fig. 18 Radial concentration profiles at the end of the afterburner chamber (test condition A).

%, which is in accordance with Fig. 18. An axial concentration profile at the combustion chamber centerline for oxygen and carbon dioxide is shown in Fig. 19. The oxygen is consumed towards the end of the combustor and, therefore, its content is diminishing. The concentration of carbon dioxide is rising.

No hydrogen and insignificant amounts of hydrocarbons have been found during these experiments. This can be explained by the test conditions, which were locally not fuel-rich enough to form larger amounts of H_2. Some experiments were carried out in which the tip of the probe was placed in the borehole inside the fuel wall, so the gas sample was sucked off the fuel surface. In this case, hydrocarbons were found, especially at $z/D_3 = 0.6$. Even in this situation, small amounts of oxygen were also detected.

A comparison of the temperature and concentration profiles across the recirculation zone at $z/D_3 = 0.6$ shows that there is a region between the wall and the separating streamline where the local concentrations of the species do not change very rapidly. However, the temperature varies more than 750°C across the recirculation zone. This leads to the observation that the recirculation zone may be partially homogeneous in concentrations but not homogeneous in temperature. The formation of a recirculation zone is very important to flame stabilization. Some models[25,26] interpret bluff body or dump combustor flame stabilization based on the theory of premixed flames by well-stirred reactors. These experiments show that these models may not be applicable in recirculation zones with mass transfer from the wall, since the conditions for a homogeneous well-stirred region are not or only partially fulfilled.

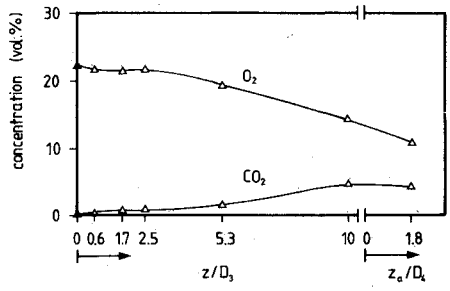

Fig. 19 Axial concentration profiles (test condition A).

Furthermore, the results of the experiments show that there is no complete mixing in the combustion channel. In the middle, there is a zone which is relatively low in temperature and high in oxygen content. The two layers mix partially towards the end of the combustion chamber. Closer to the wall, there is a layer of combustion products with a high temperature level. For complete mixing and combustion, an afterburner chamber of sufficient length or other mixing devices are needed, especially if stoichiometric air/fuel mixture ratios are required.

Conclusions

The significant conclusions of the present study can be summarized as follows: 1) In the recirculation zone the combustion process takes place mainly in the shear layer of the incoming air flow. Fuel-rich gases are recirculated and react with air near the inlet. This leads to maximum temperatures in the shear layer. 2) The recirculation zone is not a homogeneous well-stirred region and seems to be fuel-rich. Especially the temperature variation across the recirculation zone is very large. Therefore, well-stirred reactor models may not be applicable. 3) Small amounts of oxygen are still found at the wall.

It was also found that 1) the flame position in the redeveloping boundary layer is dependent on the air mass flux and the type of fuel regression behavior and is slightly dependent on inlet temperature; and 2) the flow in the combustor can be separated into two regions: a colder zone in the core, which is air-rich, and a zone of combustion products closer to the wall. The two zones mix incompletely along the combustion chamber.

References

[1]Das, A. N., "Dominating Role of Degradation Kinetics in the Heterogeneous Combustion of Cross-Linked Polymers," *Combustion and Flame,* Vol. 42, 1981, pp. 35-43.

[2]Baial, S. K. and Sriramulu, A. N., "Kinetic Factors in Heterogeneous Combustion of Cross-Linked Polymers," *AIAA Journal,* Vol. 12, Oct. 1974, pp. 1413-1415.

[3]Joulain, P., Most, J. M., Sztal, B., and Vantelon, J. P., "Theoretical and Experimental Study of Gas-Solid Combustion in Turbulent Flow," *Combustion Science and Technology,* Vol. 15, 1977, pp. 225-241.

[4]Joulain, P., Most, J. M., Fuseau, Y., and Sztal, B., "Influence of Coupled Convection, Conduction and Radiation Heat Transfer on the Burning of Plastics," *Seventeenth Symposium (International) on Combustion,* The Combustion Institute, Pittsburgh, 1979, pp. 1041-1051.

[5]Mady, C. J., Hickey, P. Y., and Netzer, D. W., "Combustion Behavior of Solid-Fuel Ramjets," *Journal of Spacecraft and Rockets,* Vol. 15, May-June 1978, pp. 131-132.

[6]Marxman, G. and Gilbert, M., "Turbulent Boundary Layer Combustion in the Hybrid Rocket," *Ninth Symposium (International) on Combustion,* Academic Press, N.Y., 1963, pp. 371-383.

[7]Marxman, G. A., "Combustion in the Turbulent Boundary Layer on a Vaporizing Surface," *Tenth Symposium (International) on Combustion,* The Combustion Institute, Pittsburgh, 1965, pp. 1337-1349.

[8]Rabinovitch, B., "Regression Rates and the Kinetics of Polymer Degradation," *Tenth Symposium (International) on Combustion,* The Combustion Institute, Pittsburgh, 1965, pp. 1393-1403.

[9]Kumar, R. N. and Stickler, D. B., "Polymer-Degradation Theory of Pressure-Sensitive Hybrid Combustion," *Thirteenth Symposium (International) on Combustion,* The Combustion Institute, Pittsburgh, 1971, pp. 1059-1072.

[10]Helman, D., Wolfshtein, M., and Manheimer-Timnat, Y., "Theoretical Investigation of Hybrid Rocket Combustion by Numerical Methods," *Combustion and Flame,* Vol. 22, 1974, pp. 171-190.

[11]Stevenson, C. A. and Netzer, D. W., "Primitive-Variable Model Applications to Solid Fuel Ramjet Combustion," *Journal of Spacecraft and Rockets,* Vol. 18, Jan.-Feb. 1981, pp. 89-94.

[12]Smoot, L. D. and Price, C. F., "Regression Rates of Nonmetalized Hybrid Fuel Systems," *AIAA Journal,* Vol. 3, Aug. 1965, pp. 1408-1413.

[13]Smoot, L.D. and Price, C. F., "Regression Rates of Metalized Hybrid Fuel Systems," *AIAA Journal,* Vol. 4, May 1966, pp. 910-915.

[14]Schadow, K. C., Cordes, H. F., and Chieze, D. J., "Experimental Studies of Combustion Processes in a Tubular Combustor with Fuel Addition Along the Wall," *Combustion Science and Technology,* Vol. 19, 1978, pp. 51-57.

[15]Holve, D. J. and Sawyer, R. F., "Diffusion Controlled Combustion of Polymers," *Fifteenth Symposium (International) on Combustion,* The Combustion Institute, Pittsburgh, 1977, pp. 351-361.

[16]Pitz, W. J., Brown, W. J., and Sawyer, R. F., "The Structure of a Polyethylene Opposed Flow Flame," *Eighteenth Symposium (International) on Combustion,* The Combustion Institute, Pittsburgh, 1981, pp. 1871-1879.

[17]Blazowski, W. S., Cole, R. B., and McAlevy, R. F., "Linear Pyrolysis of Various Polymers Under Combustion Conditions," *Fourteenth Symposium (International) on Combustion,* The Combustion Institute, Pittsburgh, 1973, pp. 1177-1186.

[18]Wooldridge, C. F. and Muzzy, R. J., "Measurement in a Turbulent Boundary Layer with Porous Wall Injection and Combustion," *Tenth Symposium (International) on Combustion,* The Combustion Institute, Pittsburgh, 1965, pp. 1351-1361.

[19]Jones, J. W., Isaacson, L. K., and Vreeke, S., "A Turbulent Boundary Layer with Mass Addition Combustion and Pressure Gradients," *AIAA Journal,* Vol. 9, Sept. 1971, pp. 1762-1768.

[20]Ramachandra, A. and Raghunandan, B. N., "An Analysis of a Boundary Layer Diffusion Flame over a Porous Flat Plate in a Confined Flow," *Combustion Science and Technology,* Vol. 38, 1984, pp. 59-73.

[21]Kaskan, W. E., "The Dependence of Flame Temperature on Mass Burning Velocity," *Sixth Symposium (International) on Combustion,* Reinhold, NY, 1957, pp. 134-143.

[22]Kent, J. H., "A Noncatalytic Coating for Platinum-Rhodium Thermocouples," *Combustion and Flame,* Vol. 14, 1970, pp. 279-282.

[23]Peterson, R. C. and Laurendeau, N. M., "The Emittance of Yttrium-Beryllium Oxide Thermocouple Coating," *Combustion and Flame,* Vol. 60, 1985, pp. 279-284.

[24]Banna, S. M. and Branch, M. C., "Gas Chromatographic Determination of Nitrogenious Species in Combustion Products," *Combustion Science and Technology,* Vol. 24, 1980, pp. 15-22.

[25]Longwell, J. P., Frost, E. E., and Weiss, M. A., "Flame Stability in Bluff Body Recirculation Zones," *Industrial and Engineering Chemistry,* Vol. 45, 1953, pp. 1629-1634.

[26]Curran, E. T., "An Investigation of Flame Stability in a Coaxial Dump Combustor," Air Force Institute of Technology, OH, Ph.D. Thesis, 1979.